Role of interfacial charge in the piezoelectric properties of ferroelectric 0-3 composites

C. K. Wong[a)]
Department of Applied Physics, The Hong Kong Polytechnic University, Hong Kong, China

F. G. Shin
Department of Applied Physics, Materials Research Center and Center for Smart Materials, The Hong Kong Polytechnic University, Hong Kong, China

(Received 1 June 2004; accepted 8 November 2004; published online 19 January 2005)

We investigated the effects of compensating charges (at the inclusion-matrix interface) on the piezoelectric properties of ferroelectric 0-3 composites. Our previously developed model [C. K. Wong, Y. M. Poon, and F. G. Shin, J. Appl. Phys. **90**, 4690 (2001)] has been extended to include the additional contribution from the deformation of the inclusion particles due to the applied stress in the piezoelectric measurement. The relative significance of this contribution is mainly determined by the amount of compensating interfacial charge, which is significantly governed by the degrees of poling of the constituent materials in the composite sample. This model provides an explanation to an anomaly in the piezoelectric coefficients of 0-3 composite samples with the matrix and inclusion phases polarized in opposite directions. Explicit expressions in closed form have been derived for the effective d_{33}, d_{31}, and d_h coefficients. After taking into consideration the degree of poling of the constituents and the effects of the compensating interfacial charges, theoretical predictions show good agreement with published experimental data. Goodness of fit is not limited to low volume concentration of inclusions. © *2005 American Institute of Physics*. [DOI: 10.1063/1.1845587]

I. INTRODUCTION

Ferroelectric composites have been a subject of interest for many years because ferroelectrics have many device applications.[1] However, single-phase ferroelectric materials invariably have some inherent limitations for certain applications. These materials may be combined to form composites, taking advantage of the beneficial properties while canceling or limiting the undesirable ones. Ferroelectric composites with polymer matrix loaded with ceramic inclusions of 0-3 connectivity are probably the most commonly investigated. In characterizing the piezoelectric properties of a ferroelectric sample or composite, the piezoelectric d coefficients such as d_{31}, d_{33}, and d_h are measured. The gross piezoelectric properties of a composite are mainly dictated by the piezoelectric properties of the constituents and their volume ratio. In addition, the structure of interconnection for the different phases in a composite also plays a major role in determining its effective properties. For the design and application, theoretical models can be used to predict or evaluate the performance of a composite under study. In the past, many theories and models have been proposed for the prediction of the effective piezoelectric properties of ferroelectric composites.[2–11] Some approaches are simple which lead to elegant expressions, while some others which adopt a more rigorous approach must be computed by difficult numerical algorithms. A comprehensive review can be found in Ref. 11.

Previously, we have derived some explicit expressions for the effective piezoelectric coefficients for ferroelectric 0-3 composites.[9,10] Fairly good agreement with experimental results has been obtained. On the other hand, the existence of finite conductivity in materials allows free charges to accumulate at the inclusion-matrix interface.[12] The consideration of the depletion of interfacial charge is essential to understand some interesting polarization switching results[12] and in the poling of ferroelectric composites.[13] To impart piezoelectric activities, ferroelectrics must be subjected to a poling process for a certain duration to align the spontaneous polarization in the material(s). The duration should be sufficient for free charges to accumulate at the interface, to counteract the depolarization field, and to stabilize the polarization of the inclusion particles. The existence of interfacial charge in a poled composite sample is thus essential in this context but its implications may not be limited only to the poling behavior. Since poling imparts piezoelectric and pyroelectric activities, interfacial charge may also affect such properties in a composite. The effect on the piezoelectric properties of ferroelectric 0-3 composites has not been examined before.

Theoretical predictions of the piezoelectric coefficients of 0-3 composite samples with parallel-poled ferroelectric constituents have been amply examined in the literature and generally good agreement with experimental data has been obtained. However, quite unsatisfactory predictions often occur for composite samples with oppositely poled constituents.[10,14] Experimental plots of piezoelectric coefficient versus ceramic volume fraction always show a broad valleylike trend (such as illustrated in Ref. 14), which cannot be explained by previous models. We believe that this anomaly is related to interfacial charge effect. In this article, we attempt to investigate the effect of interfacial charge on the piezoelectric properties of ferroelectric composites of a

a)Electronic mail: wongck.a@polyu.edu.hk

dispersion of spherical inclusions in a continuous matrix. The deformation of the inclusion volume and hence the charged interface due to applied stress in piezoelectric measurement is also taken into consideration. Explicit expressions for the piezoelectric d_{31}, d_{33}, and d_h coefficients have been derived. Compared to our previously derived analytical expressions (for d_{31}, d_{33}, and d_h),[9] which assume no interfacial charge, the new set of expressions contains a new term describing the coupled effects of the interfacial charge and the change in inclusion volume fraction. Our theoretical predictions compare reasonably well with published experimental results of d_{33} for lead zirconate titanate/vinylidene fluoride-trifluoroethylene copolymer [PZT/P(VDF-TrFE)],[14] and d_{31} for lead zirconate titanate/polyvinylidene fluoride (PZT/PVDF),[2,15] covering both small and medium high ceramic volume fractions as well as different poling conditions. The anomalous phenomenon in the oppositely poled composite samples is naturally explained by this model. We will demonstrate that the contribution arising from the change in inclusion volume fraction is enhanced by the existence of interfacial charge.

II. THEORY

To find the effective piezoelectric d coefficients of a 0-3 composite of two ferroelectric phases, we will first obtain the solution of effective polarization of the ferroelectric composite, given the external electric field. Then the change of polarization due to the external applied stresses will be considered. The result can be manipulated to obtain expressions for the d_{31}, d_{33}, and d_h coefficients.

A. Effective polarization of a composite in dilute limit

Suppose the composite is subjected to an electric field in the z direction, in which case we only need to be concerned with the electric field and polarization in the "3" direction. We first write the volumetric average electric displacement for the ferroelectric constituent materials in the composite as[12]

$$\begin{cases} \langle D_{3i}\rangle = \langle P_{3i}\rangle + \varepsilon_i\langle E_{3i}\rangle \\ \langle D_{3m}\rangle = \langle P_{3m}\rangle + \varepsilon_m\langle E_{3m}\rangle, \end{cases} \tag{1}$$

where the angular brackets denote volume-averaged fields enclosed. D denotes electric displacement, P is polarization, ε is permittivity, and E is electric field. Subscripts i and m denote "inclusion" and "matrix," respectively.

Consider the single inclusion problem of a ferroelectric sphere surrounded by a ferroelectric matrix medium with a uniform electric field applied along the z direction far away from the inclusion. The boundary-value problem gives the following equation:[12]

$$\langle D_{3i}\rangle + 2\varepsilon_m(\langle E_{3i}\rangle - \langle E_{3m}\rangle) = \langle D_{3m}\rangle - q_0. \tag{2}$$

In Eq. (2), we have assumed that both constituent materials are uniformly polarized and that the homogeneously polarized sphere is covered with surface charge of density q_0 at the pole along the polarizing direction ($\theta=0$) with a distribution given by $q_0\cos\theta$.

For a composite comprising a dilute suspension of spherical particles uniformly distributed in the matrix material, the volumetric averages of the electric field and electric displacement are[2,9]

$$\begin{cases} \langle E_3\rangle = \phi\langle E_{3i}\rangle + (1-\phi)\langle E_{3m}\rangle \\ \langle D_3\rangle = \phi\langle D_{3i}\rangle + (1-\phi)\langle D_{3m}\rangle, \end{cases} \tag{3}$$

where ϕ is the volume fraction of the inclusion phase. Using Eqs. (1)–(3), we obtain, after some algebraic manipulation,

$$\langle D_3\rangle = \varepsilon\langle E_3\rangle + \langle P_3\rangle, \tag{4}$$

where

$$\varepsilon = \varepsilon_m\frac{(\varepsilon_i + 2\varepsilon_m) + 2\phi(\varepsilon_i - \varepsilon_m)}{(\varepsilon_i + 2\varepsilon_m) - \phi(\varepsilon_i - \varepsilon_m)}, \tag{5}$$

$$\langle P_3\rangle = \phi L_E\langle P_{3i}\rangle + (1-\phi)\overline{L_E}\langle P_{3m}\rangle + \phi(1-\phi)(L_E - \overline{L_E})q_0, \tag{6}$$

and

$$L_E = \frac{3\varepsilon_m}{(1-\phi)\varepsilon_i + (2+\phi)\varepsilon_m}, \tag{7}$$

$$\overline{L_E} = \frac{1-\phi L_E}{1-\phi} = \frac{\varepsilon_i + 2\varepsilon_m}{(1-\phi)\varepsilon_i + (2+\phi)\varepsilon_m}. \tag{8}$$

Note that Eq. (5) is identical to the well-known Maxwell–Wagner formula for the effective permittivity,[16] and Eq. (6) is a simple formula for the effective polarization of a ferroelectric composite. The latter can be used for analyzing the remanent polarization P_r of the composite [i.e., the effective polarization at $\langle E_3\rangle=0$]. When $\langle E_3\rangle=0$ and the polarization in the constituents are fully compensated by the free-surface charges so that $\langle E_{3i}\rangle=\langle E_{3m}\rangle=0$, $\langle P_{3i}\rangle$ and $\langle P_{3m}\rangle$ become P_{ri} and P_{rm}, respectively. Thus

$$P_r = \phi L_E P_{ri} + (1-\phi)\overline{L_E}P_{rm} + \phi(1-\phi)(L_E - \overline{L_E})q_0, \tag{9}$$

where using Eqs. (1) and (2), $q_0=P_{rm}-P_{ri}$. The state with interfacial charge fully compensating the polarizations is believed to be a natural steady state of the composite after poling, the development of which is allowed by the finite conductivity of the constituents. Simulations in previous works have demonstrated that this is the case and so we shall be consistently applying this condition in the present discussion.[13,17]

B. Effective piezoelectric coefficients of a composite in dilute limit

The polarization of a ferroelectric material will be influenced by temperature (pyroelectricity) and stress (piezoelectricity). In this work, we only focus on the piezoelectric effect. Suppose the composite is subjected to tensile stresses in the x, y, and z directions simultaneously. The change in polarization due to the stresses in the constituents can be written as

$$\begin{cases} \Delta\langle P_{3i}\rangle = d_{31i}\langle\sigma_{xxi}\rangle + d_{32i}\langle\sigma_{yyi}\rangle + d_{33i}\langle\sigma_{zzi}\rangle \\ \Delta\langle P_{3m}\rangle = d_{31m}\langle\sigma_{xxm}\rangle + d_{32m}\langle\sigma_{yym}\rangle + d_{33m}\langle\sigma_{zzm}\rangle, \end{cases} \tag{10}$$

where d_{31}, d_{32}, and d_{33} are the piezoelectric coefficients and $\langle\sigma_{xxm}\rangle$ represents the volume-averaged stress in the x direction within the matrix material, and so forth.

In a previous article, we have considered the elasticity problem of a composite with spherical inclusions subjected to external stresses σ_{xx}, σ_{yy}, and σ_{zz} and obtained[9]

$$\begin{pmatrix} \langle\sigma_{xxi}\rangle \\ \langle\sigma_{yyi}\rangle \\ \langle\sigma_{zzi}\rangle \end{pmatrix} = \begin{pmatrix} L_T^{\parallel} & L_T^{\perp} & L_T^{\perp} \\ L_T^{\perp} & L_T^{\parallel} & L_T^{\perp} \\ L_T^{\perp} & L_T^{\perp} & L_T^{\parallel} \end{pmatrix} \begin{pmatrix} \sigma_{xx} \\ \sigma_{yy} \\ \sigma_{zz} \end{pmatrix}, \tag{11}$$

$$\begin{pmatrix} \langle\sigma_{xxm}\rangle \\ \langle\sigma_{yym}\rangle \\ \langle\sigma_{zzm}\rangle \end{pmatrix} = \begin{pmatrix} \overline{L_T^{\parallel}} & \overline{L_T^{\perp}} & \overline{L_T^{\perp}} \\ \overline{L_T^{\perp}} & \overline{L_T^{\parallel}} & \overline{L_T^{\perp}} \\ \overline{L_T^{\perp}} & \overline{L_T^{\perp}} & \overline{L_T^{\parallel}} \end{pmatrix} \begin{pmatrix} \sigma_{xx} \\ \sigma_{yy} \\ \sigma_{zz} \end{pmatrix}, \tag{12}$$

where

$$L_T^{\perp} = \frac{I_T}{1-\phi(1-3I_T)} - \frac{J_T}{1-\phi(1-3J_T)}, \tag{13}$$

$$L_T^{\parallel} = \frac{I_T}{1-\phi(1-3I_T)} + \frac{2J_T}{1-\phi(1-3J_T)}, \tag{14}$$

$$\overline{L_T^{\perp}} = \frac{-\phi L_T^{\perp}}{1-\phi} = \frac{1}{3}\left[\frac{1}{1-\phi(1-3I_T)} - \frac{1}{1-\phi(1-3J_T)}\right], \tag{15}$$

$$\overline{L_T^{\parallel}} = \frac{1-\phi L_T^{\parallel}}{1-\phi} = \frac{1}{3}\left[\frac{1}{1-\phi(1-3I_T)} + \frac{2}{1-\phi(1-3J_T)}\right], \tag{16}$$

and

$$I_T = \frac{1}{3}\frac{k_i}{k_m}\frac{3k_m+4\mu_m}{3k_i+4\mu_m}, \tag{17}$$

$$J_T = \frac{5}{3}\frac{(3k_m+4\mu_m)\mu_i}{6(k_m+2\mu_m)\mu_i + (9k_m+8\mu_m)\mu_m}, \tag{18}$$

k and μ denote the bulk modulus, and shear modulus, respectively. Substituting Eqs. (11) and (12) into Eq. (10) gives

$$\begin{cases} \Delta\langle P_{3i}\rangle = \{L_T^{\parallel}d_{31i} + L_T^{\perp}(d_{32i}+d_{33i})\}\sigma_{xx} + \{L_T^{\parallel}d_{32i} + L_T^{\perp}(d_{31i}+d_{33i})\}\sigma_{yy} + \{L_T^{\parallel}d_{33i} + L_T^{\perp}(d_{31i}+d_{32i})\}\sigma_{zz} \\ \Delta\langle P_{3m}\rangle = \{\overline{L_T^{\parallel}}d_{31m} + \overline{L_T^{\perp}}(d_{32m}+d_{33m})\}\sigma_{xx} + \{\overline{L_T^{\parallel}}d_{32m} + \overline{L_T^{\perp}}(d_{31m}+d_{33m})\}\sigma_{yy} + \{\overline{L_T^{\parallel}}d_{33m} + \overline{L_T^{\perp}}(d_{31m}+d_{32m})\}\sigma_{zz}. \end{cases} \tag{19}$$

The inclusion volume fraction ϕ may also change because of the geometrical deformation of the particles under the applied stress. This in turn influences the effective polarization behavior of the composite. The change in inclusion volume fraction is (see Appendix)

$$\Delta\phi = \frac{\phi}{3}\left(\frac{L_T^{\parallel}+2L_T^{\perp}}{k_i} - \frac{1}{k}\right)(\sigma_{xx}+\sigma_{yy}+\sigma_{zz}), \tag{20}$$

where the effective bulk modulus k of the composite is given by[9]

$$k = k_m + \frac{\phi(k_i-k_m)}{1+(1-\phi)(k_i-k_m)/(k_m+4\mu_m/3)}. \tag{21}$$

Assuming permittivities ε_i and ε_m, and the charge density q_0 do not vary with applied stress, the change of $\langle D_3\rangle$ can be evaluated by (at $\langle E_3\rangle = 0$)

$$\Delta\langle P_3\rangle = \left[\frac{\partial\langle P_3\rangle}{\partial\langle P_{3i}\rangle}\Delta\langle P_{3i}\rangle + \frac{\partial\langle P_3\rangle}{\partial\langle P_{3m}\rangle}\Delta\langle P_{3m}\rangle + \frac{\partial\langle P_3\rangle}{\partial\phi}\Delta\phi\right]_{\langle P_{3i}\rangle=P_{ri},\langle P_{3m}\rangle=P_{rm}}. \tag{22}$$

Substituting Eqs. (6), (19), and (20) into Eq. (22) with some manipulation, we obtain

$$\Delta\langle P_3\rangle = d_{31}\sigma_{xx} + d_{32}\sigma_{yy} + d_{33}\sigma_{zz}, \tag{23}$$

where

$$d_{31} = d_{32} = \phi L_E\{(L_T^{\parallel}+L_T^{\perp})d_{31i} + L_T^{\perp}d_{33i}\} + (1-\phi)\overline{L_E}\{(\overline{L_T^{\parallel}}+\overline{L_T^{\perp}})d_{31m} + \overline{L_T^{\perp}}d_{33m}\} + d_{\phi}, \tag{24}$$

$$d_{33} = \phi L_E\{L_T^{\parallel}d_{33i} + 2L_T^{\perp}d_{31i}\} + (1-\phi)\overline{L_E}\{\overline{L_T^{\parallel}}d_{33m} + 2\overline{L_T^{\perp}}d_{31m}\} + d_{\phi}, \tag{25}$$

and

$$d_{\phi} = \frac{\phi}{3}\left(\frac{L_T^{\parallel}+2L_T^{\perp}}{k_i} - \frac{1}{k}\right)\left\{\left[L_E + \phi\frac{\partial L_E}{\partial\phi}\right]P_{ri} - \left[\overline{L_E} - (1-\phi)\frac{\partial\overline{L_E}}{\partial\phi}\right]P_{rm} + \Omega\right\}, \tag{26}$$

$$\Omega = \left\{(1-2\phi)(L_E-\overline{L_E}) + \phi(1-\phi)\frac{\partial(L_E-\overline{L_E})}{\partial\phi}\right\}q_0. \tag{27}$$

In the above, we have set $\langle P_{3i}\rangle = P_{ri}$, $\langle P_{3m}\rangle = P_{rm}$, $d_{31i} = d_{32i}$, and $d_{31m} = d_{32m}$. d_{ϕ} in Eqs. (24) and (25) is the contribution arising from the change in inclusion volume fraction and Ω in Eq. (26) is the interfacial charge effect embedded in d_{ϕ}. Thus the consideration of change in ϕ due to stress naturally leads to an interfacial charge effect in piezoelectric response.

The derivatives of L_E and $\overline{L_E}$ with respect to ϕ can be calculated from Eqs. (7) and (8):

$$\frac{\partial L_E}{\partial \phi} = \frac{3\varepsilon_m(\varepsilon_i - \varepsilon_m)}{[(1-\phi)\varepsilon_i + (2+\phi)\varepsilon_m]^2}, \tag{28}$$

$$\frac{\partial \overline{L_E}}{\partial \phi} = \frac{(\varepsilon_i + 2\varepsilon_m)(\varepsilon_i - \varepsilon_m)}{[(1-\phi)\varepsilon_i + (2+\phi)\varepsilon_m]^2}. \tag{29}$$

The effective hydrostatic piezoelectric d_h coefficient (defined by $d_h = d_{33} + 2d_{31}$, and similarly for inclusion and matrix) is derived by setting $\sigma_{xx} = \sigma_{yy} = \sigma_{zz}$ in Eq. (23), thus,

$$d_h = \phi L_E L_T^h d_{hi} + (1-\phi)\overline{L}_E \overline{L}_T^h d_{hm} + 3d_\phi, \tag{30}$$

where

$$L_T^h = 2L_T^\perp + L_T^\parallel = \frac{(3k_m + 4\mu_m)k_i}{(3k_m + 4\mu_m\phi)k_i + 4(1-\phi)\mu_m k_m}, \tag{31}$$

$$\overline{L_T^h} = 2\overline{L_T^\perp} + \overline{L_T^\parallel} = \frac{1 - \phi L_T^h}{1-\phi} = \frac{(3k_i + 4\mu_m)k_m}{(3k_m + 4\mu_m\phi)k_i + 4(1-\phi)\mu_m k_m}. \tag{32}$$

C. Effective polarization and piezoelectric coefficients for concentrated suspension

Equations (5)–(8) and (24)–(32) are the results based on the foregoing calculation for the dilute suspension regime. One can reexpress the L_E's and L_T's [Eqs. (7), (8), (13)–(16), (31), and (32)] in terms of the effective dielectric and elastic properties of the composite as in Ref. 9, and call the new expressions F_E's and F_T's, respectively. (This technique has been demonstrated there to give results which are applicable to higher ϕ, provided that better estimates of effective properties are available.) Thus

$$\langle P_3 \rangle = \phi F_E \langle P_{3i} \rangle + (1-\phi)\overline{F_E}\langle P_{3m} \rangle + \phi(1-\phi)(F_E - \overline{F_E})q_0, \tag{33}$$

$$d_{31} = d_{32} = \phi F_E\{(F_T^\parallel + F_T^\perp)d_{31i} + F_T^\perp d_{33i}\} + (1-\phi)\overline{F_E}\{(\overline{F_T^\parallel} + \overline{F_T^\perp})d_{31m} + \overline{F_T^\perp} d_{33m}\} + d_\phi, \tag{34}$$

$$d_{33} = \phi F_E\{F_T^\parallel d_{33i} + 2F_T^\perp d_{31i}\} + (1-\phi)\overline{F_E}\{\overline{F_T^\parallel} d_{33m} + 2\overline{F_T^\perp} d_{31m}\} + d_\phi, \tag{35}$$

$$d_h = \phi F_E F_T^h d_{hi} + (1-\phi)\overline{F_E}\,\overline{F_T^h} d_{hm} + 3d_\phi, \tag{36}$$

where

$$d_\phi = \frac{\phi}{3}\left(\frac{F_T^h}{k_i} - \frac{1}{k}\right)\left\{\left[F_E + \phi\frac{\partial F_E}{\partial \phi}\right]P_{ri} - \left[\overline{F_E} - (1-\phi)\frac{\partial \overline{F_E}}{\partial \phi}\right]P_{rm} + \Omega\right\}, \tag{37}$$

$$\Omega = \left\{(1-2\phi)(F_E - \overline{F_E}) + \phi(1-\phi)\frac{\partial(F_E - \overline{F_E})}{\partial \phi}\right\}q_0, \tag{38}$$

and

$$F_E = \frac{1}{\phi}\frac{\varepsilon - \varepsilon_m}{\varepsilon_i - \varepsilon_m}, \tag{39}$$

$$\overline{F_E} = \frac{1 - \phi F_E}{1-\phi} = \frac{1}{1-\phi}\frac{\varepsilon_i - \varepsilon}{\varepsilon_i - \varepsilon_m}, \tag{40}$$

$$\frac{\partial F_E}{\partial \phi} = \frac{\phi(\partial\varepsilon/\partial\phi) - (\varepsilon - \varepsilon_m)}{\phi^2(\varepsilon_i - \varepsilon_m)}, \tag{41}$$

$$\frac{\partial \overline{F_E}}{\partial \phi} = \frac{(\varepsilon_i - \varepsilon) - (1-\phi)(\partial\varepsilon/\partial\phi)}{(1-\phi)^2(\varepsilon_i - \varepsilon_m)}, \tag{42}$$

$$F_T^\perp = \frac{1}{\phi}\left\{\frac{1}{3}\frac{k^{-1} - k_m^{-1}}{k_i^{-1} - k_m^{-1}} - \frac{1}{3}\frac{\mu^{-1} - \mu_m^{-1}}{\mu_i^{-1} - \mu_m^{-1}}\right\}, \tag{43}$$

$$F_T^\parallel = \frac{1}{\phi}\left\{\frac{1}{3}\frac{k^{-1} - k_m^{-1}}{k_i^{-1} - k_m^{-1}} + \frac{2}{3}\frac{\mu^{-1} - \mu_m^{-1}}{\mu_i^{-1} - \mu_m^{-1}}\right\}, \tag{44}$$

$$\overline{F_T^\perp} = \frac{-\phi F_T^\perp}{1-\phi} = \frac{1}{1-\phi}\left\{\frac{1}{3}\frac{k_i^{-1} - k^{-1}}{k_i^{-1} - k_m^{-1}} - \frac{1}{3}\frac{\mu_i^{-1} - \mu^{-1}}{\mu_i^{-1} - \mu_m^{-1}}\right\}, \tag{45}$$

$$\overline{F_T^\parallel} = \frac{1 - \phi F_T^\parallel}{1-\phi} = \frac{1}{1-\phi}\left\{\frac{1}{3}\frac{k_i^{-1} - k^{-1}}{k_i^{-1} - k_m^{-1}} + \frac{2}{3}\frac{\mu_i^{-1} - \mu^{-1}}{\mu_i^{-1} - \mu_m^{-1}}\right\}, \tag{46}$$

$$F_T^h = \frac{1}{\phi}\frac{k^{-1} - k_m^{-1}}{k_i^{-1} - k_m^{-1}}, \tag{47}$$

$$\overline{F_T^h} = \frac{1 - \phi F_T^h}{1-\phi} = \frac{1}{1-\phi}\frac{k_i^{-1} - k^{-1}}{k_i^{-1} - k_m^{-1}}. \tag{48}$$

Theoretical predictions given by Eqs. (33)–(36) require the values of the permittivity, bulk modulus, and shear modulus of the composite. Sometimes the dielectric and elastic properties of the composite are not measured together with the piezoelectric properties. In such cases, we can follow the same technique as in our previous articles.[9,10] For the effective permittivity ε, the Bruggeman formula[18]

$$\frac{\varepsilon_i - \varepsilon}{\varepsilon^{1/3}} = (1-\phi)\frac{\varepsilon_i - \varepsilon_m}{\varepsilon_m^{1/3}} \tag{49}$$

is used. For the effective bulk modulus k, Eq. (21) gives a good approximation for a composite with spherical inclusions.[19] For the effective shear modulus μ, explicit bounds may be employed. Following Christensen,[20] the lower bound μ_l.

TABLE I. Properties of constituents for PZT/P(VDF-TrFE) 0–3 composites adopted for the calculations in Figs. 1–3.

	$\varepsilon/\varepsilon_0$ [a]	Y [b] (GPa)	ν [c]	P_r [c] (μC/cm^2)	d_{33} [a] (pC/N)	$-d_{31}$ [b] (pC/N)
PZT	1116	71	0.31	35	410	175
P(VDF-TrFE)	9.5	1.4	0.392	5.6	−37	−16

[a]Reference 14.
[b]Reference 10.
[c]Reference 17.

$$\mu_l = \mu_m \left\{ 1 + \frac{15(1-\nu_m)(\mu_i/\mu_m - 1)\phi}{7 - 5\nu_m + 2(4-5\nu_m)[\mu_i/\mu_m - (\mu_i/\mu_m - 1)\phi]} \right\} \tag{50}$$

given by Hashin and Shtrikman[21] for arbitrary phase geometry is adopted in our prediction. In Eq. (50), ν_m is Poisson's ratio of the matrix phase. We adopt for the upper bound μ_u Hashin's formula for spherical inclusion geometry,[19] which may be rewritten as

$$\mu_u = \mu_m \left[1 + \left(\frac{\mu_i}{\mu_m} - 1 \right) \frac{\beta}{\alpha + \beta\eta} \phi \right], \tag{51}$$

where

$$\begin{cases} \alpha = \dfrac{42}{5\mu_m} \dfrac{\mu_m - \mu_i}{1 - \nu_m} \phi(\phi^{2/3} - 1)^2 \\ \beta = [(7 - 10\nu_i) - (7 - 10\nu_m)\vartheta]4\phi^{7/3} + 4(7 - 10\nu_m)\vartheta \\ \eta = \dfrac{\mu_i}{\mu_m} + \dfrac{7 - 5\nu_m}{15(1-\nu_m)}\left(1 - \dfrac{\mu_i}{\mu_m}\right) + \dfrac{2(4-5\nu_m)}{15(1-\nu_m)}\left(1 - \dfrac{\mu_i}{\mu_m}\right)\phi \\ \vartheta = \dfrac{(7 + 5\nu_i)\mu_i + 4(7 - 10\nu_i)\mu_m}{35(1-\nu_m)\mu_m}. \end{cases} \tag{52}$$

Since the effective shear modulus contains upper bound μ_u and lower bound μ_l, each prediction of the d_{31} and d_{33} coefficients [Eqs. (34) and (35), respectively] gives a pair of lines.

In summary, Eqs. (24), (25), and (30) are used for the prediction of effective piezoelectric coefficients d_{31}, d_{33}, and d_h, respectively, in dilute limit. For higher ϕ, Eqs. (34)–(36) are used accordingly. When $d_\phi = 0$, they reduce to the expressions of our previous model.[9] In Sec. III we will show that the Ω term (interfacial charge effect) in Eqs. (26) and (37) plays a significant role in the effect of the change in ϕ under stress.

III. RESULTS AND DISCUSSION

In this section, theoretical predictions based on the foregoing expressions are compared with the experimental data of Ng *et al.*[14] for d_{33} of PZT/P(VDF-TrFE), and experimental data of Furukawa *et al.*[2] and Furukawa[15] for d_{31} of PZT/PVDF composites. The properties of the constituents adopted for the calculations are shown in Tables I–III for the experimental system of Ng *et al.*, Furukawa *et al.*, and Furukawa, respectively. ε_0, Y, and ν in the tables denote permittivity of vacuum, Young's modulus, and Poisson's ratio, respectively.

TABLE II. Properties of constituents for PZT/PVDF 0–3 composites adopted for the calculations in Fig. 4.

	$\varepsilon/\varepsilon_0$ [a]	Y [a] (GPa)	ν [b]	P_r (μC/cm^2)	d_{33} (pC/N)	$-d_{31}$ [a] (pC/N)
PZT	1700	36	0.3	33[c]	400[d]	180
PVDF	12.9	1.3	0.4	0.1	−0.8	−0.3

[a]Reference 2.
[b]Reference 10.
[c]Reference 22.
[d]Reference 9.

Y and ν may be transformed to k and μ by using $k = Y/(3-6\nu)$ and $\mu = Y/(2+2\nu)$. In the experiments of Ng *et al.*, d_{33} measurements are given for two different poling conditions: both the ceramic and copolymer phases are polarized in the same direction (group I), and the ceramic and copolymer phases polarized in opposite directions (group II).

Figure 1 shows the comparison of theoretical predictions with the d_{33} values of the group-I composites of the PZT/P(VDF-TrFE) system of Ng *et al.*[14] In Fig. 1(a), the pair of solid lines is based on our previous model,[9] which corresponds to $d_\phi = 0$ in Eq. (35) of the present model. The theoretical line is higher than the experimental values for $\phi < 0.5$. When the d_ϕ term with $q_0 = 0$ is included in Eq. (35) (i.e., consideration of volume deformation effect only), the improvement in the prediction is only minimal with the solid and dashed lines in Fig. 1(a) nearly overlapping. However, when the full Eq. (35) is used (i.e., with consideration of interfacial charge effect included), then the improvement can be considerable. The comparison shows that the prediction now [dotted line in Fig. 1(a)] agrees better with the experimental values.

In a ferroelectric ceramic/polymer composite, the permittivity of the ceramic is normally much higher than that of the polymer, thus the electric field acting on the ceramic phase would be much lower than that on the matrix phase, thus achieving a high degree of poling in the ceramic phase is fairly difficult. Ng *et al.* measured the poling ratio ζ_i in the inclusion phase and their results revealed that ζ_i was in the range of 44%–70% in their samples. Also, Chan *et al.* reported a similar degree of poling in the inclusion phase in their PZT/P(VDF-TrFE) composites.[23] Moreover, simulation of poling in a PZT/P(VDF-TrFE) system showed that, if the poling time was shorter than the relaxation time of the composite, the remanent polarization of the ceramic phase could be as low as 10% of that of a fully polarized PZT sample

TABLE III. Properties of constituents for PZT/PVDF 0–3 composites adopted for the calculations in Fig. 5.

	$\varepsilon/\varepsilon_0$ [a]	Y [b] (GPa)	ν [c]	P_r (μC/cm^2)	d_{33} [c] (pC/N)	$-d_{31}$ [a] (pC/N)
PZT	1900	36	0.3	33[d]	450	180
PVDF	14	1.3	0.4	0	0	0

[a]Reference 15.
[b]Reference 2.
[c]Reference 10.
[d]Reference 22.

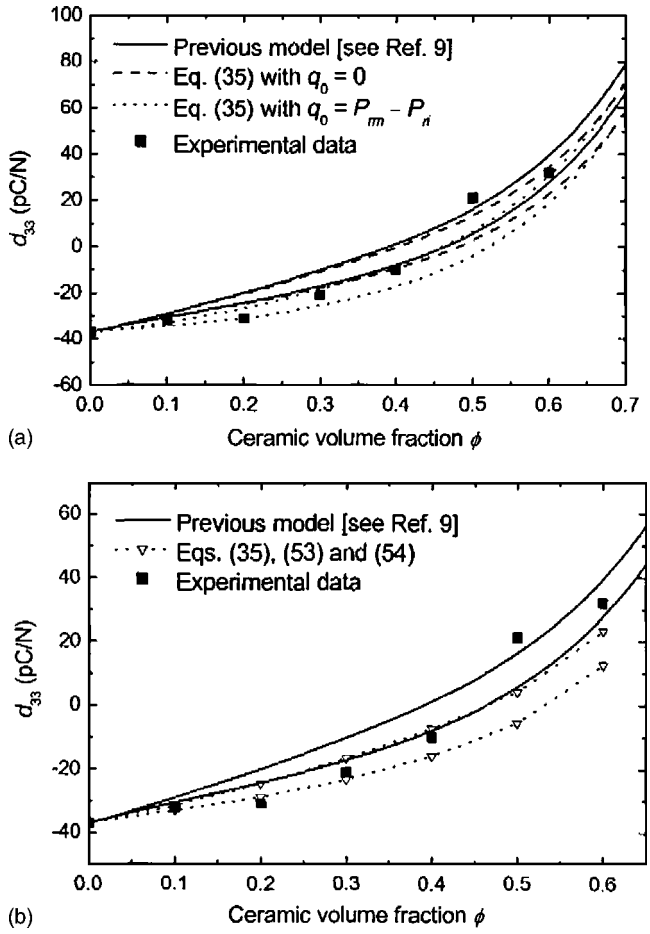

FIG. 1. Theoretical predictions by a previous model (Ref. 9) and Eq. (35), (a) with/without the effect of interfacial charge; (b) taking into account the variation of poling ratio ζ_i, are compared with the experimental data of Ng *et al.* (see Ref. 14) for the d_{33} constant of PZT/P(VDF-TrFE) composites with the ceramic and copolymer phases polarized in the same direction.

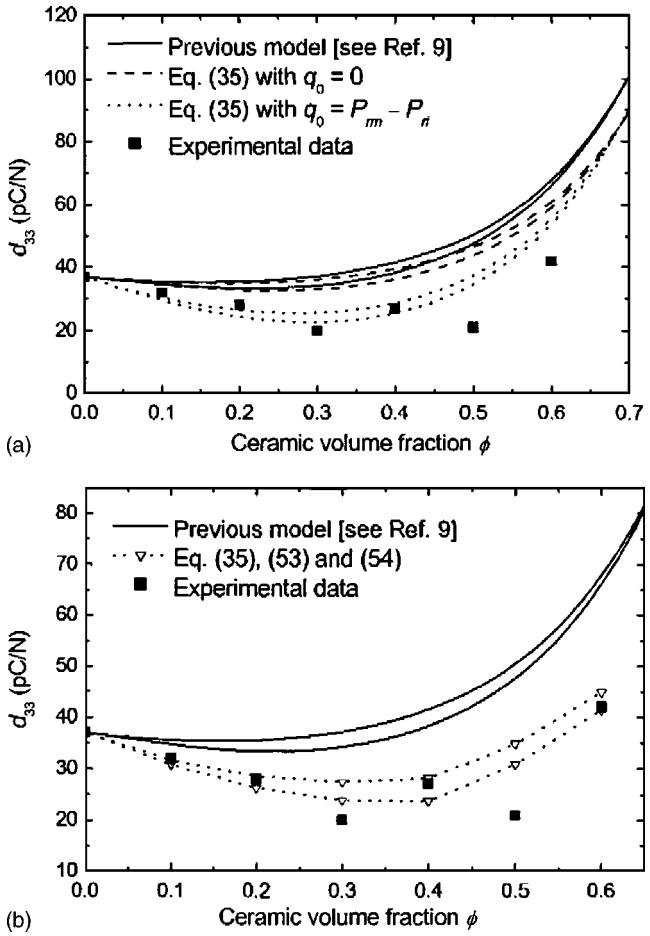

FIG. 2. Theoretical predictions by a previous model (Ref. 9) and Eq. (35), (a) with/without an effect of interfacial charge; (b) taking into account the variation of poling ratio ζ_i, are compared with the experimental data of Ng *et al.* (see Ref. 14) for the d_{33} constant of PZT/P(VDF-TrFE) composites with the ceramic and copolymer phases polarized in opposite directions.

while the copolymer phase was almost fully polarized.[17] We can include the effect of poling ratio into Eq. (35) by relating the degree of poling ζ_i to P_{ri} as

$$\zeta_i \equiv P_{ri}/P_{ri}^f, \tag{53}$$

where the superscript f denotes "fully poled." The experimental ζ_i generally varies with the ceramic volume fraction ϕ and influences the piezoelectric properties of the ceramic material. We follow our previous assumption that the piezoelectric coefficient of the inclusion is directly proportional to its P_{ri} and can, therefore, be written as[13]

$$\begin{cases} d_{31i} = (P_{ri}/P_{ri}^f) d_{31i}^f \\ d_{33i} = (P_{ri}/P_{ri}^f) d_{33i}^f, \end{cases} \tag{54}$$

where d_{31i}^f and d_{33i}^f denote the piezoelectric coefficients of a fully polarized ceramic. In Ref. 14, $\zeta_i(\phi=1)$ was reported as 0.74. The measured d_{33i} and d_{31i} listed here in Table I should not be treated as fully poled values, the latter should be $d_{31i}^f = 554$ pC/N and $d_{31i}^f = -236$ pC/N. Assuming the copolymer phase was fully polarized, and using Eqs. (35), (53), and (54) with the values of ζ_i adopted for the respective ϕ (listed in Ref. 14), comparison between our theoretical prediction [dotted line in Fig. 1(b)] and the experimental data is shown in Fig. 1(b). Apart from the largest $\phi(=0.6)$, predictions based on Eq. (35) show similar trends as the dotted lines in Fig. 1(a), i.e., both give equally good agreement with the experimental data, but better than the predictions of the previous model.

Continuing with the data of Ng *et al.*, Fig. 2(a) shows the comparison with the d_{33} values of group-II composites (both the ceramic and copolymer are polarized, but in opposite directions). In Fig. 2(a), we first consider the simpler case where the constituents are fully polarized. As in Fig. 1(a), the pair of predicted lines given by our previous model has higher values than the experimental data, and here the discrepancy is much larger than that in the group-I samples (constituents polarized in the same direction). The pair of lines from Eq. (35) with $q_0 = 0$ (neglecting interfacial charge effect) gives some improvement, but is still quite far away from the experimental data. The dotted lines in Fig. 2(a) include the interfacial charge effect in Eq. (35) and significant improvement of agreement with the experimental data is achieved, except for the two samples with higher ϕ's. It seems that the effect of interfacial charge really makes a difference. In the past, the discrepancy between predictions and the experimental data in the group-II samples has been suggested to be due to insufficient poling.[10,14] This hypoth-

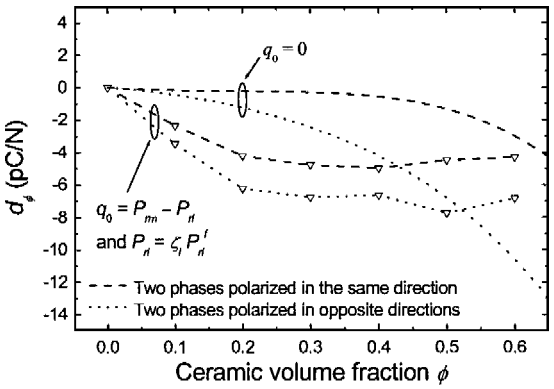

FIG. 3. Theoretical predictions by Eq. (37) of the PZT/P(VDF-TrFE) composite system of Ng *et al.* (see Ref. 14). Different poling conditions have been shown for the predictions with $[q_0=P_{rm}-P_{ri}$ and ζ_i is given by Eq. (53)] and without $[q_0=0]$ the effects of interfacial charge and poling ratio in the inclusion phase.

esis can be examined in the present study by consideration of Eqs. (53) and (54) in Eq. (35). Figure 2(b) shows the prediction of Eq. (35) with the measured ζ_i and it is evident that further improvement is obtained. Our new theoretical prediction now gives a trend which more or less agrees with the measured values. The existence of a d_{33} valley in a broad ϕ range has also been observed from the experimental data of Zeng *et al.* for PZT/P(VDF-TrFE) with oppositely poled constituents.[24] From the modeled results, we believe that this feature is explained by the present model.

Note that the interfacial charge q_0 contributes to d_{33} differently for different poling conditions. The same degree of poling in the constituents gives a higher q_0 in the group-II samples than in group-I samples. Figure 3 shows the profile of d_ϕ's vs ϕ. It is seen that even when the interfacial charge effect is neglected $(q_0=0)$, d_ϕ contributes more to the group-II samples.

Summing up, with interfacial charge considered, the model suggested in this article yields significant effects for oppositely poled samples (Fig. 2), but only minimal effects for parallel-poled samples (Fig. 1). Thus the interfacial charge correction term does not affect in a noticeable way the goodness of fit already obtained by many existing models for parallel-poled systems (although it may lead to even better results as shown in Fig. 1), while for oppositely poled systems, which may not have been fitted well by existing models, the new correction term does have a noticeable positive effect.

Concerning the PZT/PVDF system of Furukawa *et al.*,[2] since $\phi \leqslant 0.21$ for all their composite samples, we adopted the d_{31} expression for the dilute limit [Eq. (24)]. Figure 4(a) shows the comparison of Eq. (24) with the d_{31} values reported. The case with $d_\phi=0$ [solid line in Fig. 4(a)] reduces back to the model we developed previously,[9] which prediction is smaller than the experimental values. With $q_0=0$ in d_ϕ in Eq. (24), the increment of the predicted values of d_{31} is only negligible [volume deformation effect only, dashed line in Fig. 4(a)]. However, the inclusion of interfacial charge effect can dramatically improve the prediction. Since Furukawa *et al.* have not given the degrees of poling ζ_i for their composite samples, we show in Fig. 4(a) the effects of different poling ratios ζ_i. We can make use of the plotted lines in the figure to estimate ζ_i of the inclusions in the different composite samples. It is found that $\zeta_i(\phi=0.05)\approx 0.3$, $\zeta_i(\phi=0.1)$ and $\zeta_i(\phi=0.13)$ range between 0.4 and 0.5, and $\zeta_i(\phi=0.21)$ is very close to 0.5. As stated above, the degree of ceramic poling at small ϕ is generally limited, thus the magnitude of these ζ_i's are thought to be quite reasonable.

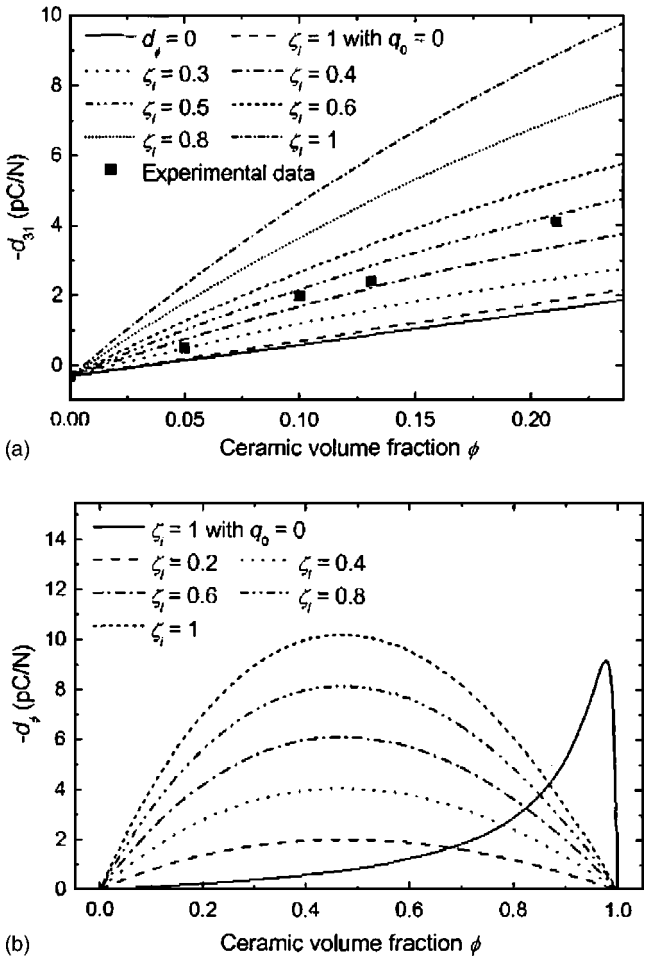

FIG. 4. Theoretical predictions by (a) a previous model (Ref. 9) $(d_\phi=0)$ and Eq. (24) are compared with the experimental data of Furukawa *et al.* (see Ref. 2) for the d_{31} constant of PZT/PVDF composites; (b) Eq. (26) with varying degrees of the poling ratio ζ_i.

The magnitude of the effects of the deformation of inclusion volume as well as the coupled interfacial charge contribution vary with ϕ. Figure 4(b) shows the variations of d_ϕ [Eq. (26)] with the ceramic volume fraction. When fully poled and $q_0=0$ [solid line in Fig. 4(b)], d_ϕ is negligible at small ϕ and its increment with ϕ is very slow until the volume fraction reaches extremely high values. When $q_0=P_{rm}-P_{ri}$ [other lines in Fig. 4(b)], d_ϕ is largest in magnitude at about $\phi=0.45$, and smallest at either low or high values of ϕ. If $\zeta_i<1$, the profile of d_ϕ vs ϕ is flattened by decreasing ζ_i. On the other hand, all d_ϕ's have the same sign as d_{31}, thus the d_ϕ term in Eq. (24) always increases the magnitude of d_{31}.

Furukawa also reported the d_{31} constant for PZT/PVDF composites of higher ceramic volume fraction in a later article.[15] Figure 5(a) shows the comparison between the experimental data and the theoretical predictions obtained from

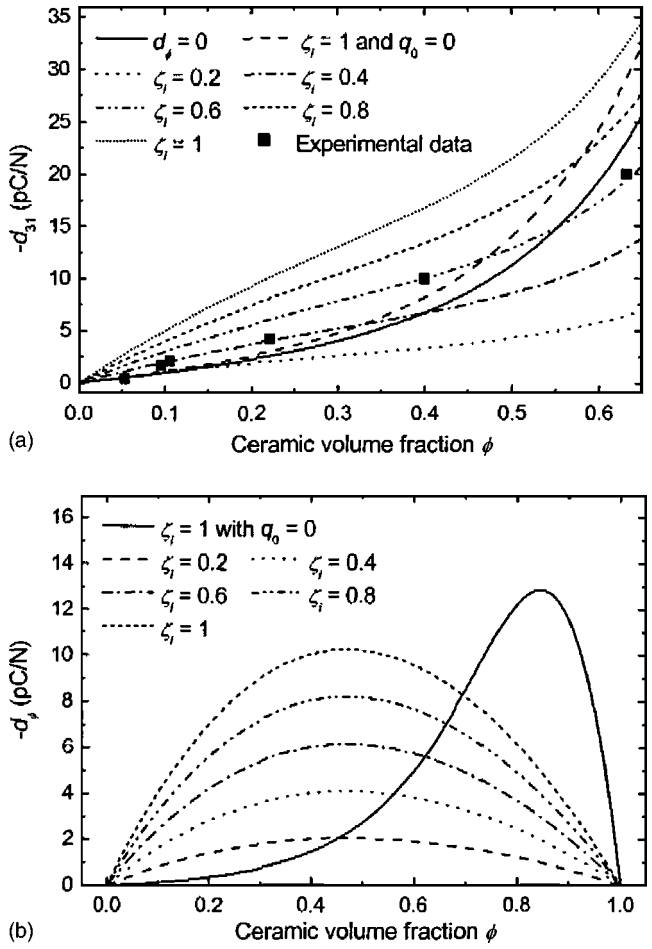

FIG. 5. Theoretical predictions by (a) a previous model (Ref. 9) ($d_\phi=0$) and Eq. (34) are compared with the experimental data of Furukawa (see Ref. 14) for the d_{31} constant of PZT/PVDF composites; (b) Eq. (37) with varying degrees of the poling ratio ζ_i.

Eq. (34) with $d_\phi=0$ (i.e., previous model), $q_0=0$ and $\zeta_i=1$ (i.e., consideration of volume deformation effect only), and $q_0=P_{rm}-P_{ri}$ of varying degrees of ζ_i. For simplicity, only Eq. (34) with μ_l [Eq. (50)] is shown. The set of predictions by Eq. (34) with μ_u [Eq. (51)] will have slightly higher d_{31} magnitudes but insufficient to make a real difference. Without interfacial charge effects [solid ($d_\phi=0$) and dashed ($q_0=0$) lines in Fig. 5(a)], the additional contribution due to the change of ϕ displaces the solid line a little. Nevertheless, the contribution from d_ϕ with $q_0=0$ is higher for a medium high ϕ. Both predictions are slightly smaller than the measured values for $\phi<0.6$. Similar to Fig. 4(a), predictions with interfacial charge effect [Eq. (34) with $q_0=P_{rm}-P_{ri}$] are shown for a varying degree of ζ_i. Comparing the theoretical lines with the measured values gives estimations of ζ_i at different ϕ. We found that $\zeta_i(\phi\approx0.05)\approx0.2$, $\zeta_i(\phi\approx0.1)$ is slightly less than 0.4 while $\zeta_i(\phi=0.22)$ and $\zeta_i(\phi=0.4)\approx0.4$ and 0.6, respectively, and $\zeta_i(\phi=0.63)$ is larger than 0.6. All in all, these values are quite typical and they suggest that the degrees of poling in Furukawa's experimental system progressively improve as the ceramic volume fraction increases.

Variation of d_ϕ [Eq. (37)] with ϕ is shown in Fig. 5(b). For Eq. (34) with $\zeta_i=1$ and $q_0=0$, the general profile of d_ϕ vs ϕ is similar to that predicted by Eq. (26) [shown in Fig. 4(b)], except that the value of ϕ now reveals a maximum d_ϕ at about 0.85. This difference is thought to be the result of the consideration of higher volume fraction in Eq. (49), while the formula for the effective bulk modulus [Eq. (21)] is identical for a high or low ϕ treatment. For the case with $q_0=P_{rm}-P_{ri}$, irrespective to the adopted value of ζ_i, all predictions with q_0 in Fig. 5(b) demonstrate similar features as in Fig. 4(b).

Sometimes d_ϕ can also be quite significant at high ϕ even when $q_0=0$ [solid line in Fig. 5(b)]. In reality, it is difficult to fabricate 0–3 composite samples for $\phi>0.6$. Therefore, from the experience of Figs. 4 and 5, we can usually ignore the pure volume deformation part in d_ϕ for most composites. Another point worth noting is that Eqs. (26) and (37) always give the same values for the same composite sample, irrespective of whether the piezoelectric d_{33} or d_{31} is calculated. Normally for ceramic/polymer composite, $|d_{33i}-d_{33m}|>|d_{31i}-d_{31m}|$, thus the contribution due to the same ζ_i is larger for the case of d_{31}. Since the signs of d_{33} and d_{31} coefficients are opposite, the same d_ϕ which displaces the effective $-d_{31}$ [Eqs. (24) and (34)] "upward" at some ϕ will displace the effective d_{33} [Eqs. (25) and (35)] "downward."

In the literature, many sophisticated models have also been suggested for the piezoelectricity of ferroelectric composites. Although difficult numerical computation schemes must invariably be employed to get predictions of the effective piezoelectric properties, they were claimed to faithfully reproduce the piezoelectric response of a composite. However, most of the studies are confined to systems with only the inclusions poled or both constituents poled in parallel directions.

Piezoelectric effects with oppositely poled constituents are rarely discussed. The present relatively simple model incorporates the coupled effects of the deformation of inclusion volume under stress, interfacial charge, and the degree of poling in the piezoelectric response of ferroelectric 0–3 composites, and it seems to provide a good understanding of the measured piezoelectric coefficients for various poling conditions. Equations (24), (25), (34), and (35) are the results of the model. For rough estimations of d's, Eqs. (37) and (38) might be combined and approximated as

$$d_\phi \approx \frac{\phi}{3}\left(\frac{F_T^h}{k_i}-\frac{1}{k}\right)\left\{(1-2\phi)(F_E-\overline{F_E}) + \phi(1-\phi)\frac{\partial(F_E-\overline{F_E})}{\partial\phi}\right\}q_0, \tag{55}$$

because the contribution from the terms associated with P_{ri} and P_{rm} in Eq. (37) is generally much smaller than Ω for a ceramic/polymer composite.

IV. CONCLUSIONS

In conclusion, we have included the effect of the change of inclusion deformation with the contribution from interfacial charge in the prediction of piezoelectric properties. New explicit expressions have been derived for d_{33}, d_{31}, and d_h coefficients which are suitable for both dilute and concen-

trated suspensions. Interfacial charge effect in piezoelectricity will not show up if one solely considers its existence in Eq. (2) (without consideration of volume change). The magnitude of d_ϕ [Eqs. (37) and (38)] is mainly dictated by q_0 which has an origin in the poling process. Comparison with the experimental results of PZT/P(VDF-TrFE) given by Ng *et al.*[14] indicates that the interfacial charge effect may be responsible for the discrepancy between the measured values and predictions by previous models when the constituents are poled in opposite directions. The present model may be used to estimate the degrees of poling ζ_i in the ceramic phase. It is found that the experimental results of PZT/PVDF by Furukawa[15] show an increasing trend of ζ_i with ϕ.

ACKNOWLEDGMENT

This work was partially supported by the Center for Smart Materials of The Hong Kong Polytechnic University.

APPENDIX

The change of inclusion volume fraction is obtained from the differential of ϕ. Hence,

$$\Delta\phi = \phi(\gamma_i - \gamma), \tag{A1}$$

where γ is the volumetric strain (summation of tensile strain components, i.e., $\gamma = e_{xx} + e_{yy} + e_{zz}$ for the composite and similarly for γ_i for the inclusions). To facilitate the derivation of the piezoelectric d coefficients, the strain components should be transformed to stress components.

The relations between stresses in the constituents and in the composite are given by Eqs. (11) and (12). From Hooke's law, we can write

$$\begin{pmatrix} \langle\sigma_{xxi}\rangle \\ \langle\sigma_{yyi}\rangle \\ \langle\sigma_{zzi}\rangle \end{pmatrix} = \frac{1}{3}\begin{pmatrix} 3k_i + 4\mu_i & 3k_i - 2\mu_i & 3k_i - 2\mu_i \\ 3k_i - 2\mu_i & 3k_i + 4\mu_i & 3k_i - 2\mu_i \\ 3k_i - 2\mu_i & 3k_i - 2\mu_i & 3k_i + 4\mu_i \end{pmatrix}\begin{pmatrix} \langle e_{xxi}\rangle \\ \langle e_{yyi}\rangle \\ \langle e_{zzi}\rangle \end{pmatrix}, \tag{A2}$$

$$\begin{pmatrix} \sigma_{xx} \\ \sigma_{yy} \\ \sigma_{zz} \end{pmatrix} = \frac{1}{3}\begin{pmatrix} 3k + 4\mu & 3k - 2\mu & 3k - 2\mu \\ 3k - 2\mu & 3k + 4\mu & 3k - 2\mu \\ 3k - 2\mu & 3k - 2\mu & 3k + 4\mu \end{pmatrix}\begin{pmatrix} e_{xx} \\ e_{yy} \\ e_{zz} \end{pmatrix}, \tag{A3}$$

and all shear stress components vanish in the present system.[9] The volumetric strain γ_i and γ can be found from Eqs. (A2) and (A3). Substituting Eq. (11) into Eq. (A2), the resulting equation together with Eq. (A3) are then used to eliminate the volumetric strains in Eq. (A1). We finally obtain

$$\Delta\phi = \frac{\phi}{3}\left(\frac{L_T^{\parallel} + 2L_T^{\perp}}{k_i} - \frac{1}{k}\right)(\sigma_{xx} + \sigma_{yy} + \sigma_{zz}). \tag{A4}$$

[1] K. Uchino, *Ferroelectric Devices* (Marcel Dekker, New York, 2000).
[2] T. Furukawa, K. Ishida, and E. Fukada, J. Appl. Phys. **50**, 4904 (1979).
[3] T. Yamada, T. Ueda, and T. Kitayama, J. Appl. Phys. **53**, 4328 (1982).
[4] N. Jayasundere, B. V. Smith, and J. R. Dunn, J. Appl. Phys. **76**, 2993 (1994).
[5] M. L. Dunn and M. Taya, Int. J. Solids Struct. **30**, 161 (1993).
[6] B. Jiang, D. N. Fang, and K. C. Hwang, Int. J. Solids Struct. **36**, 2707 (1999).
[7] C. W. Nan and G. J. Weng, J. Appl. Phys. **88**, 416 (2000).
[8] H. Zewdie, Bulletin of the Chemical Society of Ethiopia 12, 159 (1998).
[9] C. K. Wong, Y. M. Poon, and F. G. Shin, J. Appl. Phys. **90**, 4690 (2001).
[10] C. K. Wong, Y. M. Poon, and F. G. Shin, J. Appl. Phys. **93**, 487 (2003).
[11] C. J. Dias and D. K. Das-Gupta, IEEE Trans. Dielectr. Electr. Insul. **3**, 706 (1996).
[12] C. K. Wong, Y. W. Wong, and F. G. Shin, J. Appl. Phys. **92**, 3974 (2002).
[13] Y. T. Or, C. K. Wong, B. Ploss, and F. G. Shin, J. Appl. Phys. **94**, 3319 (2003).
[14] K. L. Ng, H. L. W. Chan, and C. L. Choy, IEEE Trans. Ultrason. Ferroelectr. Freq. Control **47**, 1308 (2000).
[15] T. Furukawa, IEEE Trans. Electr. Insul. **24**, 375 (1989).
[16] J. C. Maxwell, *A Treatise on Electricity and Magnetism*, reprinted (Dover, New York, 1954), Vol. 1.
[17] K. W. Kwok, C. K. Wong, R. Zeng, and F. G. Shin, Appl. Phys. A: Mater. Sci. Process. (published online first, 2004).
[18] D. A. Bruggeman, Ann. Phys. (Leipzig) **24**, 636 (1935).
[19] Z. Hashin, J. Appl. Mech. **29**, 143 (1962).
[20] R. M. Christensen, *Mechanics of Composite Materials* (Wiley, New York, 1979), Chap. 4.
[21] Z. Hashin and S. Shtrikman, J. Mech. Phys. Solids **11**, 127 (1963).
[22] T. Furukawa, K. Suzuki, and M. Date, Ferroelectrics **68**, 33 (1986).
[23] H. L. W. Chan, Y. Chen, and C. L. Choy, Integr. Ferroelectr. **9**, 207 (1995).
[24] R. Zeng, K. W. Kwok, H. L. W. Chan, and C. L. Choy, J. Appl. Phys. **92**, 2674 (2002).